

Dust emissivity in the submm/mm SCUBA and SIMBA observations of Barnard 68

S. Bianchi¹, J. Gonçalves^{2,3}, M. Albrecht⁴, P. Caselli², R. Chini⁴, D. Galli², and M. Walmsley²

¹ CNR-Istituto di Radioastronomia – Sezione di Firenze, Largo E. Fermi 5, 50125 Firenze, Italy

² INAF-Osservatorio Astrofisico di Arcetri, Largo E. Fermi 5, 50125 Firenze, Italy

³ Centro de Astronomia e Astrofísica da Universidade de Lisboa, Tapada da Ajuda, 1349-018 Lisboa, Portugal

⁴ Astronomisches Institut der Ruhr-Universität Bochum, Universitätsstr. 150, 44780 Bochum, Germany

Received 21 December 2002 / Accepted 18 January 2003

Abstract. We have observed the dark cloud Barnard 68 with SCUBA at 850 μm and with SIMBA at 1.2 mm. The submillimetre and millimetre dust emission correlate well with the extinction map of Alves et al. (2001). The $A_V/850 \mu\text{m}$ correlation is clearly not linear and suggests lower temperatures for the dust in the inner core of the cloud. Assuming a model for the temperature gradient, we derive the cloud-averaged dust emissivities (normalised to the V -band extinction efficiency) at 850 μm and 1.2 mm. We find $\kappa_{850 \mu\text{m}}/\kappa_V = 4.0 \pm 1.0 \times 10^{-5}$ and $\kappa_{1.2 \text{ mm}}/\kappa_V = 9.0 \pm 3.0 \times 10^{-6}$. These values are compared with other determinations in this wavelength regime and with expectations for models of diffuse dust and grain growth in dense clouds.

Key words. radiation mechanisms: thermal – dust, extinction – ISM: clouds, individual objects: Barnard 68 – submillimetre – radio continuum: ISM

1. Introduction

Despite being a fundamental parameter in Far Infrared, Submillimetre and Millimetre astronomy, few measurements of the dust emissivity¹ are available (for a review, see Alton et al. 2000; James et al. 2002). The submm/mm dust emissivity is particularly important for star formation studies. Since molecules are known to deplete inside prestellar cores (Bergin et al. 2002), dust emission may represent the best tracer of the gas density distribution just prior to the onset of gravitational collapse. Thus measurements in the submm/mm define the initial conditions from which a core collapses to form a star. Alternatively, the density distribution can be mapped through extinction, by measuring the near-infrared colour excess towards giant stars in the background of a cloud (Lada et al. 1994). High resolution and S/N maps can be obtained for objects in the foreground of dense stellar fields (Alves et al. 2001).

This is the case for the dark cloud Barnard 68, a starless globule seen in the foreground of the Galactic Bulge. Alves et al. (2001) have produced a high resolution extinction map of the cloud, measuring the $H - K$ colour excess of nearly 4000 stars in its background. In this paper, we compare the

extinction map with observations of submm/mm dust emission of similar resolution. Observations are described in Sect. 2. In Sect. 3 we derive the dust emissivity from the correlation between emission and extinction (in a way similar to Kramer et al. 1998, 2003). We will also adopt a temperature gradient within the cloud, which was derived from a model of dust heating. Finally, the derived emissivities are compared with other estimates from literature in Sect. 4.

2. Submm/mm observations

Barnard 68 was observed with the Submillimetre Common User Bolometer Array (SCUBA) at the JCMT (Holland et al. 1999) and with the SEST Imaging Bolometer Array (SIMBA; Nyman et al. 2001). Both instruments have hexagonal arrays of 37 bolometers: SCUBA can observe in the submm at 850 μm with $FWHM = 14.5''$ while SIMBA operates at 1.2 mm and has a beamsize of $24''$.

SCUBA observed an area of $5' \times 5'$ around Barnard 68 in scan-map mode, chopping within the field of view. The resultant image is convolved with the chop function, which is removed by means of Fourier Transform analysis. The Emerson II technique is used to minimise the noise (Jenness et al. 1998): six scans of the field are made with different chop throws ($20''$, $30''$ and $65''$ in RA and Dec). In total, we coadded eight sets of scans, six observed in March/June 2002 and two in July 1998 (the latter retrieved from the SCUBA Archive). Standard data reduction was performed with the dedicated package SURF. After flat-fielding and masking of

Send offprint requests to: S. Bianchi,
e-mail: sbianchi@arcetri.astro.it

¹ The emissivity proper is the emission [absorption] cross section normalized to the geometrical cross section of a dust grain. Other authors prefer the cross section normalized to the mass of the grain. Both quantities are the same when normalised to the analogous quantity for V -band extinction.

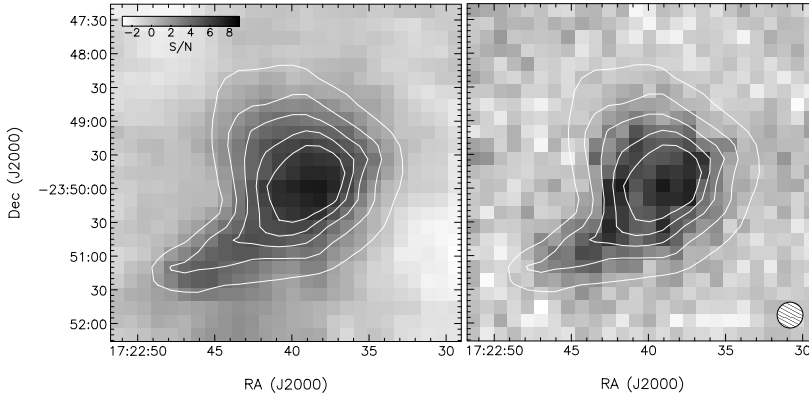


Fig. 1. SCUBA map at $850\ \mu\text{m}$ (left) and SIMBA map at $1.2\ \text{mm}$ (right) of Barnard 68, with superimposed A_V contours. The A_V and SCUBA maps have been smoothed to match the SIMBA resolution ($FWHM = 24''$; the beamsize is shown on the right image). All images have been resampled to a pixel size of $12''$. The field of view is $5' \times 5'$. A_V contours start at 4 mag and are spaced by 4 mag. For both images, the grayscale in units of S/N .

noisy bolometers, a baseline was removed from each bolometer. Maps were corrected for atmospheric extinction (the zenith optical depth was $\tau_{850} = 0.12, 0.15, 0.3$ in the 1998 run and in the March/June 2002 runs, respectively) and for correlated sky noise. Calibration was obtained from scan-maps of Uranus. The final map has a sky noise of $20\ \text{mJy beam}^{-1}$ ($1-\sigma$), equivalent to $3.5\ \text{MJy sr}^{-1}$ for the SCUBA beamsize.

SCUBA scan-maps suffer from large scale undulations in the background of the source, which are due both to the poor sampling of small spatial frequencies and to uncertainties in the baseline removal (see, e.g. Visser et al. 2002). On our image, the undulations show up as a negative background around the source, of the order of the sky noise. We subtracted a mean background estimated on several sky apertures. The results of the next section are not significantly changed by the subtraction. The integrated flux at $850\ \mu\text{m}$ inside the $2-\sigma$ isophote is $F_{850\ \mu\text{m}} = 4.0 \pm 1.0\ \text{Jy}$. SCUBA also took maps with the $450\ \mu\text{m}$ array. The signal at this wavelength is poor, because of the background fluctuations and of the larger sky opacity ($\tau_{450} \approx 0.5$ for the best data). The peak emission is detected at $3-\sigma$ level ($1-\sigma = 200\ \text{mJy beam}^{-1}$; beamsize $FWHM = 10''$) and it is not possible to conduct the surface brightness analysis described in Sect. 3. Nevertheless, we could estimate the integrated flux, which is $F_{450\ \mu\text{m}} = 13 \pm 4\ \text{Jy}$.

SIMBA observations were taken in fast scanning mode, without using a wobbling secondary mirror (Nyman et al. 2001). The bolometer array scans the observed area with a speed of $80''\ \text{s}^{-1}$ in azimuth and a scan-to-scan separation of $8''$ in elevation. Spatial frequencies are converted into temporal frequencies and the sky signal is filtered out with a low-cut filter. Each map of Barnard 68 covers $600'' \times 312''$ in azimuth and elevation, and takes 7 min to complete. Barnard 68 was observed during June and October 2001. A total of 118 maps were coadded together, for a total integration time of 13.8 hours. The mean zenith optical depth is $\tau_{1.2} = 0.16$.

Data were reduced with the software package MOPSI by R. Zylka. After deconvolution according to the frequency passband, subtracting a baseline to each scan, correcting for sky opacity and gain elevation the correlated sky noise fluctuations and artifacts due to electronics were removed. All maps of Barnard 68 were rebinned in a single image, with pixel size $8''$. In an iterative way, a preliminary image was used as source model to improve the removal of correlated noise. Uranus maps were used to calibrate the data. Night-to-night

fluctuations suggest a calibration uncertainty of 20% ($1-\sigma$). The final SIMBA image of Barnard 68 has a residual noise of $5.5\ \text{mJy beam}^{-1}$ ($1-\sigma$), equivalent to $0.36\ \text{MJy sr}^{-1}$ for the SIMBA resolution. The integrated flux is $F_{1.2\ \text{mm}} = 0.7 \pm 0.2\ \text{Jy}$.

The emission is compared to the extinction map of Alves et al. (2001) (the measured NIR colour excess has been converted to A_V using a standard reddening law; Rieke & Lebofsky 1985). All images have been smoothed to the SIMBA resolution, registered together (pointing accuracy is better than a few arcsec for the submm/mm observations) and resampled to a common pixel size of $12''$. Figure 1 shows the final SCUBA (left) and SIMBA (right) images, with superimposed A_V contours.

3. Analysis

The morphology of the extinction and emission maps in Fig. 1 is quite similar. Dust emission with $S/N > 3$ traces regions with extinction $A_V > 6$ and $A_V > 10$, in the SCUBA and SIMBA images, respectively. In analogy with extinction, emission comes from a round region with a south east tail. At $1.2\ \text{mm}$, there are hints for a secondary emission peak. In Fig. 2 we show the pixel-to-pixel correlation of the emission maps with A_V . As already seen in Fig. 1, there is a clear correlation between emission and extinction. For regions with $A_V > 10$ the scatter in the correlation with the submm data is of the order of the sky noise ($1.7\ \text{MJy sr}^{-1}$ for the smoothed image). For $A_V < 10$ the scatter increases because of the (possibly hotter) south-east tail. The pixels clearly belonging to the tail can be seen in Fig. 2 around $A_V = 8$ and $I_\nu = 10\ \text{MJy sr}^{-1}$. The scatter at $1.2\ \text{mm}$ is more uniform and slightly larger than the sky noise, because of the complex central morphology. A forthcoming paper will be devoted to the analysis of the central peaks and of the south-east tail.

For optically thin radiation (as for the submm/mm emission of Barnard 68) we can write

$$I_\nu = \frac{\kappa_\nu}{\kappa_V} \times \frac{A_V}{1.086} \times \frac{\int \rho B_\nu(T) dl}{\int \rho dl}, \quad (1)$$

where T and ρ are the temperature and density of dust grains, functions of the position within the cloud, B_ν is the Planck function and the integral extends along the line of sight through the dust. In the isothermal case, the last term on the right

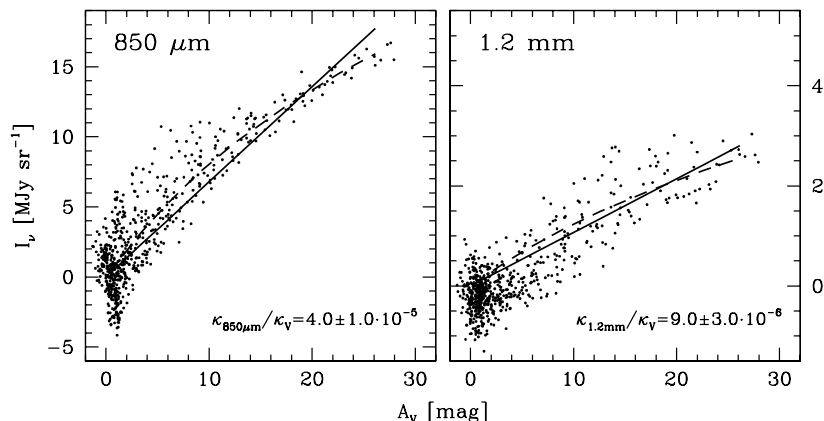


Fig. 2. Pixel to pixel correlation between dust emission and A_V extinction, at $850 \mu\text{m}$ (left) and 1.2 mm (right). The solid line is the isothermal fit, assuming a temperature $T_{\text{iso}} = 12 \text{ K}$, while the dashed line and the emissivity values refer to the temperature gradient model with external temperature $T_{\text{ext}} = 14 \text{ K}$ (see text for details). All high signal-to-noise points with $A_V > 10$ have been used for the fit.

reduces to $B_\nu(T)$. Otherwise, a knowledge of the dust temperature and density distribution is needed.

In Fig. 3 we show the Spectral Energy Distribution (SED) of Barnard 68. Our integrated fluxes at $850 \mu\text{m}$ and 1.2 mm are similar to those presented by Ward-Thompson et al. (2002), from which we took the ISOPHOT fluxes at $170 \mu\text{m}$ and $200 \mu\text{m}$. We fitted a isothermal modified blackbody to the datapoints assuming a value for β , the emissivity spectral index ($\kappa_\nu \propto \nu^\beta$). For $\beta = 1.5\text{--}2$ (Dunne & Eales 2001), we find acceptable fits for temperatures $T_{\text{iso}} = 11\text{--}13 \text{ K}$. We adopt $T_{\text{iso}} = 12 \pm 2 \text{ K}$ ($1\text{-}\sigma$) for the isothermal case, incorporating in the broad error the large uncertainties on β . The solid line in Fig. 3 is an indicative SED for $\beta = 1.7$ and $T_{\text{iso}} = 12 \text{ K}$. Similar temperature have been previously obtained for Barnard 68 (Ward-Thompson et al. 2002; Hotzel et al. 2002). Using T_{iso} , we fitted Eq. (1) to the correlations of Fig. 2 and derived a single cloud-averaged value for the submm and mm emissivities. We obtained $\kappa_{850 \mu\text{m}}/\kappa_V = 3.5 \pm 1.0 \times 10^{-5}$ and $\kappa_{1.2 \text{ mm}}/\kappa_V = 9.0 \pm 3.0 \times 10^{-6}$. Errors were estimated with a bootstrap technique and are dominated by the uncertainty on calibration and on temperature.

The fitted correlations are shown as solid lines in Fig. 2. While the fit is acceptable at 1.2 mm , a simple linear relation is unable to reproduce well the correlation observed at $850 \mu\text{m}$ for $A_V > 20$ since the I_ν/A_V ratio decreases for increasing A_V . This is expected if the temperature in the cloud core is lower than in the external part, as a result of the dust shielding of the external radiation field (Zucconi et al. 2001). Such a trend has been observed in other clouds (see, e.g. Kramer et al. 1998). A similar behaviour could also be explained with a isothermal dust distribution, if the dust emissivity is lower in denser regions. However, models and observations suggest that emissivities increase in dense cores (Ossenkopf & Henning 1994; Kramer et al. 2003).

We derived the temperature gradient inside the cloud from an improved version of the Zucconi et al. model (Gonçalves et al., in preparation). As in Alves et al. (2001), the adopted density distribution is that for a Bonnor-Ebert sphere, a pressure confined isothermal sphere in hydrostatic equilibrium. Dust is heated by a local Interstellar Radiation Field (Galli et al. 2002). The internal dust absorption is fixed by the measured extinction and the assumed absorption law κ_ν/κ_V , for which we used the tabulated values given by

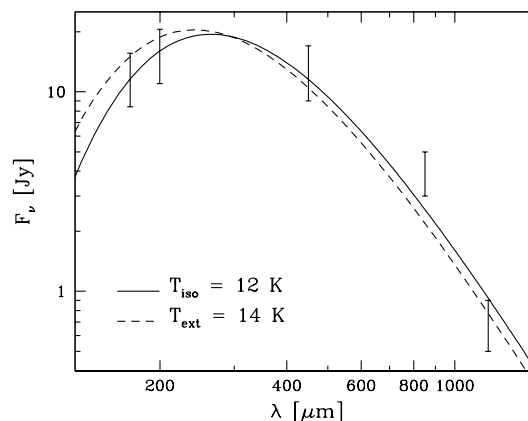


Fig. 3. SED of Barnard 68. The solid line is the isothermal model with $T_{\text{iso}} = 12 \text{ K}$. The dashed line is for the model with a temperature gradient, with $T_{\text{ext}} = 14 \text{ K}$. Both cases assume $\beta = 1.7$.

Ossenkopf & Henning (1994) for different models of dust coating/coagulation in dense clouds. While the absolute value of the temperature depends on the adopted dust model (for $\lambda > 30 \mu\text{m}$, κ_ν/κ_V increases going from bare grains to grains with ice coating up to grains that undergo coagulation), the temperature gradient is found to be relatively independent of grain characteristics, with the temperature at the truncation radius T_{ext} (0.06 pc ; Alves et al. 2001) about 1.5 times higher than the core temperature. This is because the absorption law does not change significantly with the dust model at shorter wavelengths, where most of the absorption occurs. In the following, we adopt the model radial gradient and derive T_{ext} from the data.

For the assumed density and temperature distributions, we simulated emission maps with $24''$ resolution and $12''$ pixels, in analogy with the data. The integrated SED is shown with a dashed line in Fig. 3. Again, a broad range of best fit temperatures is obtained, $T_{\text{ext}} = 12\text{--}15 \text{ K}$. We use $T_{\text{ext}} = 14 \pm 2 \text{ K}$ ($1\text{-}\sigma$). Finally, the simulated A_V vs. I_ν correlation of Eq. (1) is fitted to the observed data to derive κ_ν/κ_V . We obtained²

$$\kappa_{850 \mu\text{m}}/\kappa_V = 4.0 \pm 1.0 \times 10^{-5}$$

$$\kappa_{1.2 \text{ mm}}/\kappa_V = 9.0 \pm 3.0 \times 10^{-6}.$$

² Equivalent to $\kappa_{850 \mu\text{m}} = 1.5 \pm 0.4 \text{ cm}^2 \text{ g}^{-1}$ and $\kappa_{1.2 \text{ mm}} = 0.35 \pm 0.1 \text{ cm}^2 \text{ g}^{-1}$ (assuming grain radius $0.1 \mu\text{m}$, grain density 3 g cm^{-3} and V -band extinction efficiency 1.5; Hildebrand 1983).

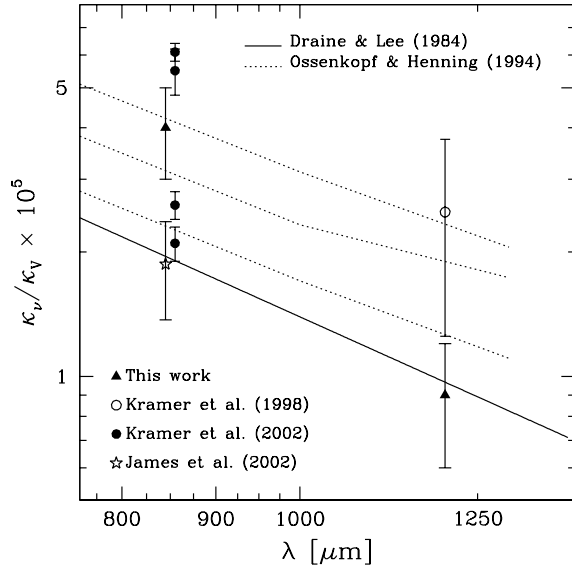


Fig. 4. Submm/mm emissivities compared with other literature estimates (details in the text). A standard ratio κ_K/κ_V (Rieke & Lebofsky 1985) has been used to derive κ_v/κ_V from Ossenkopf & Henning (1994). Data from Draine & Lee (1984) and James et al. (2002) are converted to κ_v/κ_V as in Bianchi et al. (1999) and Alton et al. (2000). Points at 850 μm have been slightly shifted in λ for ease of presentation.

These correlations are also shown in Fig. 2 with dashed lines. Although the fit to the submm data has improved, the emissivities are nearly the same as for the isothermal case.

4. Discussion

The derived submm/mm emissivities are shown in Fig. 4 together with estimates from literature. Emissivities derived from IRAS/COBE observations of diffuse Galactic dust (Boulanger et al. 1996; Bianchi et al. 1999) are within 10% of the values predicted by the popular Draine & Lee (1984) model, which is shown in Fig. 4 as a solid line. Dotted lines refer to the Ossenkopf & Henning (1994) models for bare grains, grains with a thin ice coating and grains with thin ice after coagulation has proceeded for 10^5 years in a gas with density 10^6 g cm^{-3} (from bottom to top, respectively).

James et al. (2002) derived the emissivity from a sample of local galaxies observed with SCUBA, estimating the dust mass from metals. Their value is compatible to that of Draine & Lee (1984), indicating similar properties for diffuse dust in external galaxies and in the Milky Way. Our 850 μm emissivity is higher than that of diffuse dust: a comparison with the models of Ossenkopf & Henning (1994) seems to suggest that grains in Barnard 68 possess molecular ice mantles or have coagulated into fluffy aggregates. However, $\kappa_{850 \mu\text{m}}/\kappa_V$ is within 2σ of that for bare grains. In a very recent paper, Kramer et al. (2003) measured $\kappa_{850 \mu\text{m}}/\kappa_V$ for a molecular ridge and four embedded cores in the dark cloud IC5146. Their radially averaged values of the four cores, derived assuming $\beta = 2$, range from 2.1×10^{-5} to 6.1×10^{-5} and are broadly compatible with our determination. At 1.2 mm, our emissivity is similar to that of

diffuse dust but lower than the value previously estimated by Kramer et al. (1998) on a IC5146 core.

The ratio $\kappa_{850 \mu\text{m}}/\kappa_{1.2 \text{ mm}}$ we derive implies a value for β larger than what expected from measurements on Galactic diffuse dust and on laboratory cosmic dust analogues (Mennella et al. 1998). However, the error on the ratio is large and $\beta = 2$ is still compatible (within $1-\sigma$) with our result. Contamination of the submm and mm fluxes by the $^{12}\text{CO}(3-2)$ and $^{12}\text{CO}(2-1)$ lines (Avery et al. 1987) was found to be negligible.

Clearly, more observations are needed to narrow down the errors in the determination of the emissivity. The analysis presented here has to be repeated on a large sample of objects of relatively simple morphology like Barnard 68. Only with a statistical sample will it be possible to study the variation of dust properties with the environment.

Acknowledgements. We are grateful to J. Alves, R. Cesaroni, A. Natta, C. Lada and C. Kramer (the referee) for useful comments and discussions.

References

- Alton, P. B., Xilouris, E. M., Bianchi, S., et al. 2000, *A&A*, 356, 795
- Alves, J. F., Lada, C. J., & Lada, E. A. 2001, *Nature*, 409, 159
- Avery, L. W., White, G. J., Williams, I. P., & Cronin, N. 1987, *ApJ*, 312, 848
- Bergin, E. A., Alves, J., Huard, T., & Lada, C. J. 2002, *ApJL*, 570, L101
- Bianchi, S., Davies, J. I., & Alton, P. B. 1999, *A&A*, 344, L1
- Boulanger, F., Abergel, A., Bernard, J.-P., et al. 1996, *A&A*, 312, 256
- Draine, B. T. & Lee, H. M. 1984, *ApJ*, 285, 89
- Dunne, L. & Eales, S. 2001, *MNRAS*, 327, 697
- Galli, D., Walmsley, M., & Gonçalves, J. 2002, *A&A*, 394, 275
- Hildebrand, R. H. 1983, *QJRAS*, 24, 267
- Holland, W. S., Robson, E. I., Gear, W. K., et al. 1999, *MNRAS*, 303, 659
- Hotzel, S., Harju, J., Juvela, M., Mattila, K., & Haikala, L. K. 2002, *A&A*, 391, 275
- James, A., Dunne, L., Eales, S., & Edmunds, M. G. 2002, *MNRAS*, 335, 753
- Jenness, T., Lightfoot, J. F., & Holland, W. S. 1998, in *Proc. SPIE*, 3357, Advanced Technology MMW, Radio, and Terahertz Telescopes, ed. T. G. Phillips, 548
- Kramer, C., Alves, J., Lada, C., et al. 1998, *A&A*, 329, L33
- Kramer, C., Richer, J., Mookerjee, B., Alves, J., & Lada, C. 2003, *A&A*, 399, 1073
- Lada, C. J., Lada, E. A., Clemens, D. P., & Bally, J. 1994, *ApJ*, 429, 694
- Mennella, V., Brucato, J. R., Colangeli, L., et al. 1998, *ApJ*, 496, 1058
- Nyman, L.-Å., Lerner, M., Nielbock, M., et al. 2001, *The Messenger*, 106, 40
- Ossenkopf, V. & Henning, T. 1994, *A&A*, 291, 943
- Rieke, G. H. & Lebofsky, M. J. 1985, *ApJ*, 288, 618
- Visser, A. E., Richer, J. S., & Chandler, C. J. 2002, *AJ*, 124, 2756
- Ward-Thompson, D., André, P., & Kirk, J. M. 2002, *MNRAS*, 329, 257
- Zucconi, A., Walmsley, C. M., & Galli, D. 2001, *A&A*, 376, 650